NUCLEAR SCIENCE AND TECHNIQUES **26**, 060301 (2015)

Biosorption behavior and mechanism of thorium on *Bacillus* sp. dwc-2 isolated from soil*

LAN Tu (兰图),[1] DING Cong-Cong (丁聪聪),[1,2] LIAO Jia-Li (廖家莉),[1,†]
LI Xiao-Long (李晓龙),[1] LI Xing-Liang (李兴亮),[3] ZHANG Jie (张杰),[2] ZHANG Dong (张东),[3]
YANG Ji-Jun (杨吉军),[1] LUO Shun-Zhong (罗顺忠),[3] AN Zhu (安竹),[1] WU Qi-Qi (邬琦琦),[1]
YANG Yuan-You (杨远友),[1] FENG Su (冯甦),[2] TANG Jun (唐军),[1] and LIU Ning (刘宁)[1,‡]

[1]*Key Laboratory of Radiation Physics and Technology (Sichuan University), Ministry of Education; Institute of Nuclear Science and Technology, Sichuan University, Chengdu 610064, China*
[2]*Key Laboratory of Biological Resource and Ecological Environment of the Ministry of Education, College of Life Sciences, Sichuan University, Chengdu 610064, China*
[3]*Institute of Nuclear Physics and Chemistry, CAEP, Mianyang, 621900, China*

(Received March 6, 2015; accepted in revised form May 3, 2015; published online December 20, 2015)

To develop a microbe-based bioremediation strategy for cleaning up thorium-contaminated sites, we have investigated the biosorption behavior and mechanism of thorium on *Bacillus* sp. dwc-2, one of the dominant species of bacterial groups isolated from soils in Southwest China. Thorium biosorption depended on the pH of environment, and its rapid biosorption reached a maximum of up to 10.75 mg Th per gram of the bacteria (wet wt.) at pH 3.0. The biosorption agreed bettter with Langmuir isotherm model than Freundlich model, indicating that thorium biosorption was a monolayer adsorption. The thermodynamic parameters, negative change in Gibbs free energy and positive value in enthalpy and entropy, suggested that the biosorption was spontaneous, more favorable at higher temperature and endothermic process with an increase of entropy. Scanning electron microscopy (SEM) indicated that thorium initially binded with the cell surface, while transmission electron microscopy (TEM) revealed that Th deposited in the cytoplasm and served as cores for growth of element precipitation (e.g., phosphate minerals) or by self-precipitation of hydroxides, which is probably controlled by ion-exchange, as evidenced by particle induced X-ray emission (PIXE) and enhanced proton backscattering spectrometry (EPBS). Fourier Transform Infrared (FTIR) further indicated that thorium biosorption involved carboxyl and phosphate groups and protein in complexation or electrostatic interaction. Overall results indicated that a combined electrostatic interaction-complexation-ion exchange mechanism could be involved in thorium biosorption by *Bacillus* sp. dwc-2.

Keywords: Thorium, *Bacillus* sp., Biosorption, Mechanism, Transmission electron microscopy (TEM), Particle induced X-ray emission (PIXE), Enhanced proton backscattering spectrometry (EPBS)

DOI: 10.13538/j.1001-8042/nst.26.060301

I. INTRODUCTION

The development of nuclear science and technology is accompanied with increasing scarcity of available uranium resources. As potential nuclear fuel, thorium is being explored as an alternative for reactors or in other nuclear applications [1, 2]. However, thorium has a long half life and high toxicity, and is considered as a severe ecological and public health hazard [3]. Therefore, understanding the behavior of thorium in the environment is important.

Soil is an important environmental medium with which radionuclides can interact and in which radionuclide species can undergo transformations. Microbes are an essential part of the soil ecosystem. Many are capable of growing and reproducing rapidly and tolerating extreme environmental conditions. The cells have a high surface-to-volume ratio, which can affect the valence, speciation, and chemical behavior of some elements under certain conditions, and thereby modify their mobility and toxicity through altered solubility, redox reactivity, and bioaccumulation/biosorption, etc. [4, 5]. Among these processes, biosorptive accumulation is of interest in the development of microbe-based bioremediation strategies to clean up contaminated sites. Biosorption as currently practiced, and likely be practiced in the future, has been extensively reviewed [6–15]. Compared to conventional remediation methods, which are expensive and ineffective in treating low levels of metal [4, 7, 16], biosorption is considered as a potential economically attractive alternative, being advantageous in its low operating cost, applicability to minimal volumes of chemical and/or biological sludge, and high efficiency in detoxifying dilute waste streams [17, 18]. Furthermore, biosorbent materials often have a high metal-loading capacity and in some cases are highly specific for certain elements of particular interest [19].

Exploration of the microbe-radionuclide interactions has recently gained interest, and clarification of the underlying mechanism will benefit to better devise effective and economically feasible microbial biosorption processes for contaminated sites. Biosorption of thorium was investigated using microbes such as *Rhizopus arrhizus* [1], *Citrobacter* sp. [20], *Pseudomonas* [21], *Micrococcus lu-*

* Supported by National Natural Science Foundation of China (Nos. 21071102 and 91126013), Joint Funds of China National Natural Science Foundation and China Academy of Engineering Physics (No. U1330125) and the National Fund of China for Fostering Talents in Basic Science (No. J1210004)
† liaojiali@scu.edu.cn
‡ nliu720@scu.edu.cn

teus [22], *Arthrobacter nicotianae*, *Bacillus* megaterium, and *Rhodococcus erythropolis* [23], *Streptomyces levoris* [24], *Sargassum filipendula* [25, 26], *Bacillus* sp. [27], *Cellulosimicrobium cellulans* [28], and *Agaricus bisporus* [29]. Only a few reports are available on the mechanism of thorium biosorption, hence the need of studying in more detail. Among the few reports, Tsezos and Volesky [1, 30] investigated U and Th biosorption by *Rhizopus arrhizus* and indicated that the biosorption mechanism consists of at least three processes (coordination, adsorption and precipitation). Santamaría *et al*. [31, 32] reported that thorium affects the growth and capsule morphology of *Bradyrhizobium* in liquid medium and suggested that this might be a specific defense mechanism involving thorium precipitation by extracellular polymers. Kazy *et al*. [33] investigated the chemical nature and mechanism of uranium and thorium sequestration by a *Pseudomonas* strain using transmission electron microscopy, atomic force microscopy, energy dispersive X-ray analysis, FTIR spectroscopy and X-ray diffractometry, and indicated a combined mechanism of ion exchange–complexation–microprecipitation could be involved in uranium and thorium sequestration by this bacterium.

In this paper, we evaluate the diversity of microbial communities in the aerobic zone of soil in Southwest China. *Bacillus* sp. dwc-2, a dominant bacterium at a depth of 3.5 m in this soil, is chosen to investigate its interaction with thorium, aimed at studying thorium behavior in presence of strain dwc-2 and mechanism of their interactions, so as to develop a bioremediation strategy for cleaning up thorium-contaminated sites. Scanning electron microscopy (SEM) and energy dispersive spectroscopy (EDS), transmission electron microscopy (TEM), Fourier transform infrared spectroscopy (FTIR), particle induced X-ray emission (PIXE) and enhanced proton backscattering spectrometry (EPBS) are employed to study the thorium/bacterium interaction.

II. MATERIALS AND METHODS

A. Materials and reagents

Soil samples were obtained from a disposal site planned for very low radioactive waste treatment in Southwest China. Thorium nitrate ($Th(NO_3)_4 \cdot 4\,H_2O_{(s)}$) was provided by LEA Company (France). A stock solution of Th (1 g/L) was prepared by dissolving 2.983 g of $Th(NO_3)_4 \cdot 4\,H_2O$ in 1000 mL using 2.0 mol/L HNO_3. Diluted solutions were prepared by appropriate dilution of stock solution in distilled water. All the other chemicals used in this study were of analytical grade unless stated otherwise.

All glassware for the biosorption experiments were routinely washed with 0.5 mol/L HNO_3 and rinsed extensively with distilled water to prevent interference by contaminants. The pH of each solution was measured using a digital pH meter and adjusted by the addition of 0.5 mol/L HNO_3 or 0.5 mol/L NaOH solution.

B. Strain cultivation and identification

Microbes were all extracted from soil without further treatment. Microbial communities of the samples were analyzed using spread plate method with three kinds of general medium (bacteria, fungi, and actinomycete). Pure cultures of bacteria were derived from colonies on the spread plates from the bacterial enumerations from soil samples. They were cultured in liquid medium (303.15 K, 250 mL conical flask, shaking speed: 150 r/min) consisting of (g/L): beef extract, 3; peptone, 10; NaCl, 5. The medium was adjusted to pH 7.0–7.2. After growth of 3–5 days, the bacteria were harvested by centrifugation at 4000 r/min for 10 min and washed several times with sterile water before use in an experiment. The dead cells were obtained by autoclaving at 394.15 K in a high-pressure steam sterilizer.

The bacteria were subjected to DNA extraction using the cetyltrimethylammonium bromide (CTAB) method, which was used as a template for PCR amplification of the 16S rRNA gene sequence. PCR mixtures used for amplification of bacterial sequences contained 0.75 μmol/L of each primer, 2.5 μmol/L of premixed deoxynucleoside triphosphates (dNTPs), 2.5 μL of 10×KOD buffer, 0.5 U of KOD-plus-neo DNA polymerase (TOYOBO company, Japan), 1 ng of DNA template, 1.5 μmol/L of Mg^{2+} and sterile water to a final volume of 25 μL. PCR amplification was begun with an initial denaturation at 371.15 K for 2 min, followed by 30 cycles of denaturation at 371.15 K for 10 sec, annealing at 327.15 K for 30 s, and extension at 341.15 K for 1 min. A final extension was run at 341.15 K for 1 min. The amplification products were subjected to DNA sequencing (BGI, Beijing). The sequences were subjected to a BLAST research to assess taxonomic hierarchy from NCBI (http://www.ncbi.nlm.nih.gov/), and multiple sequence alignment was performed with Clustal X version (Institut de Genetique et de Biologie Moleculaire et Cellulaire, France).

C. Biosorption experiments

Biosorption experiments were performed by a batch equilibration method. Except described otherwise, for all biosorption experiments, the biomass of 5 $g_{wet\ weight}$/L (*Bacillus* sp. dwc-2) was added to a plastic centrifuge tube containing Th with a concentration of 10 mg/L at pH 3.0. The effect of pH was investigated in the range of pH 1.0–7.0. When studying the effect of contact time, we sampled and analyzed during specific time intervals. The mixture was shaken (150 r/min) for 4 h at 303.15 K in a constant temperature shaker. A 2.0 mL-sample was then extracted from the reaction mixture, centrifuged (10 000 r/min, 5 min) at room temperature, and analyzed to measure the Th concentration in the supernatant liquid by UV-Vis spectrophotometer at 660 nm as described below.

The results were expressed as the sorption ratio (R, %) and the sorption capacity (q_e, mg metal/g biomass wet weight.). The sorption ratio and capacity were calculated as:

$$R = (1 - C/C_0) \times 100\%, \quad (1)$$

$$q_e = (C_0 - C)V/m, \quad (2)$$

where V is the sample volume (mL); C_0 is the initial thorium concentration (mg/L); C is the equilibrium or final thorium concentration (mg/L); and m is the biomass wet weight (mg).

D. Determination of thorium concentration

The concentration of Th(IV) was measured with a UV-Vis spectrophotometer (Shimadzu, UV2450) using arsenazo III reagent [34]. To a glass flask containing 1.0 mL of Th(IV) solution, 1.0 mL of 8% oxalic acid, 1.0 mL of 5% ascorbic acid, 1.0 mL of 10% urea as well as 1.0 mL of a 0.06% aqueous solution of arsenazo III were added. The final volume of the reaction mixture was accurately adjusted to 25 mL by addition of 6 mol/L HNO_3. After 20 min, the absorbance of the reaction mixture was measured in a 1 cm quartz cell at 660 nm.

E. SEM analysis

SEM (Hitachi, S4800) was used to observe the location of the adsorbed thorium ions on the bacteria. After centrifugation at 10 000 r/min for 5 min at room temperature of a suspension of bacterial cells, the cell pellet was fixed with 2.5% glutaraldehyde at 277.15 K for 4 h. The fixed cells were washed at least 3 times with distilled water, dehydrated successively in 10%, 30%, 50%, 70%, 80%, and 90% ethanol, and then placed in acetate-iso-pentalipid. Finally, the cells were dried by the critical point drying method and coated with a thin layer of Au.

F. TEM analysis

Cells of *Bacillus* sp. dwc-2 with and without Th adsorbed by them were examined by TEM (FEI, Tecnai G2 F20 S-TWIN). For this study, the cells grown in the liquid medium with and without added thorium were separated by centrifugation at 10 000 r/min for 5 min at room temperature, fixed in 2.5% glutaraldehyde in 0.1 mol/L phosphate buffer at 277.15 K for 4 h, treated with 1% OsO_4 at 277.15 K for 30 min, and then dehydrated through a graded ethanol series (10%, 30%, 50%, 70%, 80%, and 90%) for 10 min. The dehydrated samples were embedded in epoxy resins and sectioned into ultra-thin specimens. Thin specimen sections were supported on copper grids and examined using TEM.

G. FTIR analysis

The IR spectra in the 4000–400 cm^{-1} range were recorded for the original and Th-adsorbed *Bacillus* sp. dwc-2 using a FTIR (Thermo, Nicolet 6700). Cell samples were dried at 353.15 K and then prepared using the standard KBr method [35].

H. PIXE and EPBS analyses

Bacillus sp. dwc-2 grown in presence and absence of added thorium was dried at 353.15 K and pressed to form a pellet for PIXE and EPBS analyses. The PIXE and EPBS analyses were performed with 2 MeV proton beams from the Van de Graaff accelerator in the Institute of the Nuclear Science and Technology, Sichuan University. The proton beams bombarded vertically on the samples. EPBS spectra were recorded at a scattering angle of 165° by an Au(Si) detector with depletion depth of 100 μm. The proton-induced X-rays were detected at 135° by a Si(Li) detector. The EPBS and PIXE spectra were analyzed by using the computer codes SIMNRA (Max-Planck-Institut für Plasmaphysik, Germany) and GUPIXWIN (University of Guelph Guelph, Canada), respectively.

III. RESULTS AND DISCUSSION

A. Identification of bacterial isolate

By using spread plates method, the bacterial enumerations from soil samples were 4.3×10^5 cfu/g (fungi, 1.2×10^3 cfu/g; actinomycete, 6.5×10^2 cfu/g). A phylogenic tree was constructed by neighbor-joining method (Fig. 1). Multiple alignment of the phylogenic tree shows that the bacterial isolate dwc-2 is closely related and has 100% homology to *Bacillus* sp. PSM10. Therefore strain dwc-2 was identified as *Bacillus* sp. dwc-2. Its 16S rRNA sequence has been deposited in GenBank under access NO. KC508632.

B. Th biosorption by *Bacillus* sp. dwc-2

1. *Effect of pH*

Many previous reports showed that pH or acidity is an important factor influencing the biosorption of radionuclides or heavy metals by microbes [14, 18, 19]. Similarly, we found that pH had a significant effect on thorium biosorption by living and dead cells of *Bacillus* sp. dwc-2. As shown in Fig. 2(a), in 4 h, at an initial Th content of 10 mg/L, for the living cells the sorption ratio increased with pH value up to about pH 5.0; while for dead cells it declined slightly from pH 1.0 to 4.0, and increased sharply from pH 4.0 to 5.0. Without the cells (the control), thorium solution began to hydrolyze beyond pH 3.0 and completely hydrolyze at about pH 5.5. Figure 2(c) shows the distribution of thorium species computed by Visual MINTEQ 3.0, the soluble thorium species like Th^{4+} decrease, while hydrolyzed species $Th(OH)^{3+}$ and $Th(OH)_2^{2+}$ predominate [36, 37]. The

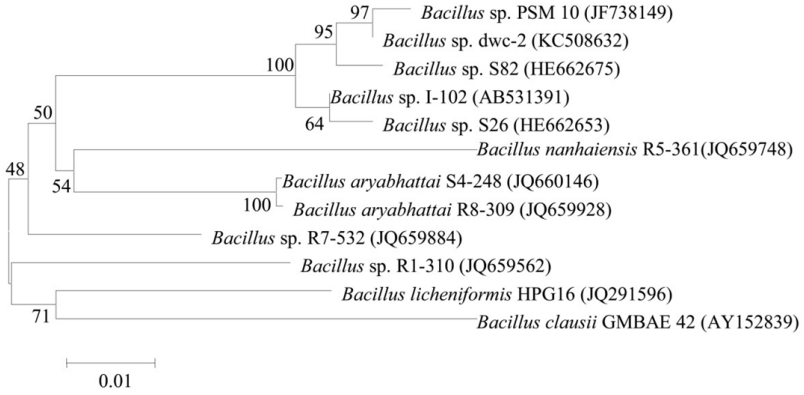

Fig. 1. Phylogenetic tree of bacterial isolate dwc-2 and related genera of *Bacillus* sp. based on 16S rRNA sequences.

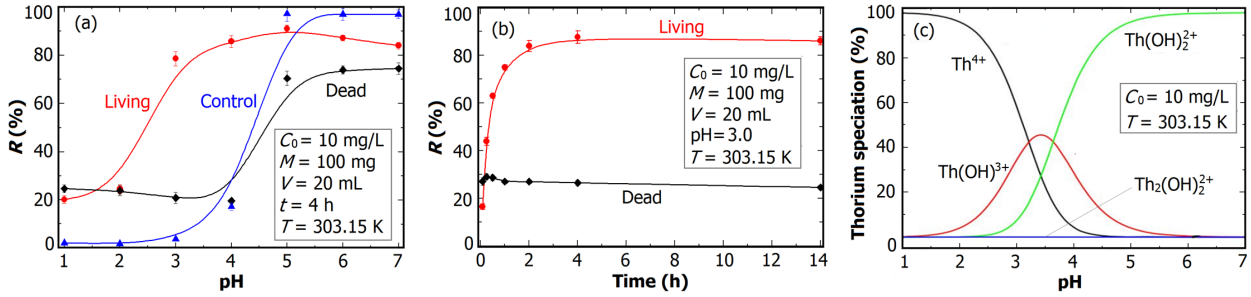

Fig. 2. (Color online) Thorium biosorption by living and dead cells of *Bacillus* sp. dwc-2, as a function of pH (a) and contact time (b); and speciation of thorium as a function of pH (c).

hydrolyzed species like $[Th(OH)_2]^{2+}$ and other polymerized thorium species have been proven to possess a greater binding affinity for the biomass functional groups than soluble Th^{4+} [21, 38]. The high biosorption of thorium on biomass at pH>5.0 can also be attributed to the partial precipitation or coprecipitation of Th(IV) owing to the predominated hydrolyzed thorium species at high pH. Thus, we set pH 3.0 for the subsequent biosorption experiments, except as otherwise described.

Based on these results, we inferred that the effect of pH on thorium biosorption involved a change in net charge on the surface of the cells. For microbes, the isoelectric point (pI) usually ranges from 2.5 to 3.5 [5]. So at higher pH than the isoelectric point, cell surface was negatively charged, and the electrostatic attraction between thorium and bacteria was enhanced. The negative charge might come from the functional groups of cell surface including carboxyl, hydroxyl and phosphate groups, etc. (see FTIR analysis, Section III C 3). Since thorium is tetravalent, it has higher affinity to the cell surface than other cations of low valence, such as K^+, Mg^{2+} and Fe^{3+} for these functional group sites. At pH values smaller than the isoelectric point, cells may be neutralized or become positively charged, explaining why the sorption ratio was low at pH 1.0–2.0. It indicated that electrostatic interaction was a major contributor to the thorium biosorption on *Bacillus* sp. dwc-2.

2. *Effect of contact time*

To further verify the biosorption behavior, we investigated the effect of contact time on thorium biosorption by the living and dead cells (Fig. 2(b)). Again, the biosorption behavior of living cells differs from that of the dead cells. For the living cells, the sorption ratio increased gradually with time and reached equilibrium within 4 h; while for the dead cells it reached equilibrium in just 5 min. This may suggest different sorption mechanisms.

Based on this result, the contact time was set to 4 h for the other biosorption experiments unless otherwise indicated. Compared with the dead bacteria, thorium biosorption of the living cells not only depended on its physical and chemical sorption, but also relied on its metabolism, thus the balance time was relatively long. Microbes adsorb and accumulate nuclides depending on metabolism, which are generally divided into two cases: 1) rely on energy and carriers to actively adsorb nuclides; and 2) rely on some materials produced by metabolism, or structural changes in the cells to passively adsorb nuclides [32]. So far, the first case is rare, and the living cells are unlikely to actively adsorb thorium depending on energy and carriers due to its chemical toxicity and radioactivity. The living cells passively adsorb thorium may rely on materials produced or structures changed by metabolism.

3. *Effect of biomass concentration and initial thorium concentration*

The effect of biomass concentration on thorium biosorption by the living bacteria was presented in Fig. 3(a). The sorption ratio increased with biomass concentration from 0.5 to 4.0 g/L, with a sharp increase of about 80%. After that, it reached a plateau. The effect of initial thorium concentration on biosorption by the living cells was shown in Fig. 3(b). The sorption capacity increased with initial thorium concentration and reached 10.75 mg/g (wet weight).

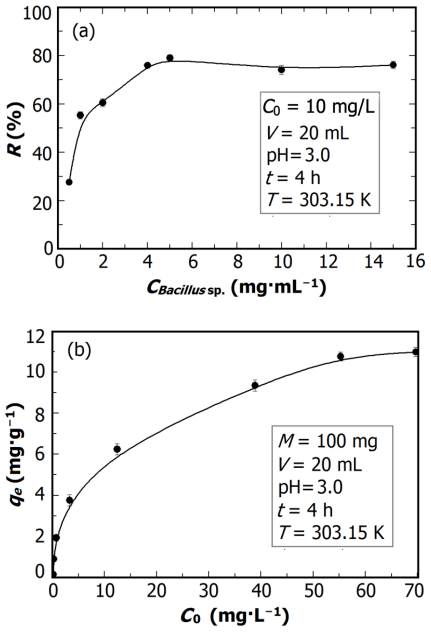

Fig. 3. Thorium biosorption by living cells of *Bacillus* sp. dwc-2 as function of biomass wet weight (a) and thorium concentration (b).

The results were evaluated by Langmuir isotherm and Freundlich isotherm. The Langmuir isotherm model assumes that the adsorbate molecules form an adsorbed layer one molecule in thickness and that all sites are equal. It can be expressed as

$$\frac{C_0}{q_e} = \frac{1}{bq_m} + \frac{C_0}{q_m}, \tag{3}$$

where q_m (mg/g) and b (L/mg) are the measure of Langmuir monolayer sorption capacity and the equilibrium constant, respectively.

The Freundlich isotherm is employed to describe heterogeneous systems, which assumes that sorbent surface sites have a spectrum of different binding energies. It is given by following equation,

$$\ln q_e = \ln K_F + \frac{1}{n} \ln C_0, \tag{4}$$

where K_F [(mg/g) (L/mg)$^{1/n}$] and n are the Freundlich constants which are related to sorption capacity of the sorbent and the intensity of sorption, respectively.

The correlation coefficients and corresponding parameters listed in Table 1 were calculated from the slopes and intercepts of the plots of $1/q_e$ versus $1/C_0$ and $\ln q_e$ versus $\ln C_0$. The experimental data fitted the Langmuir isotherm model better than the Freundlich isotherm model, indicating that the biosorption of Th formed a monolayer coverage.

4. *Thermodynamic studies*

The biosorptive thermodynamics is important to understand the biosorption mechanism of Th by the living cells of *Bacillus* sp. dwc-2. The biosorption of Th was investigated as a function of temperature. As shown in Fig. 4(a), the amounts of Th adsorbed increased with temperature, indicating that higher temperature was beneficial to the Th biosorption. The change of thermodynamic parameters of biosorption process can be acquired by Eq. (5),

$$\ln K_d = \frac{\Delta S}{R} - \frac{\Delta H}{RT}, \tag{5}$$

where K_d is the distribution coefficient (mg/g), T is the absolute temperature (K), R is the gas constant (8.314 J/(mol K)), ΔS is the change of entropy (J/(mol K)), and ΔH is the change of enthalpy (kJ/mol). The change of Gibbs free energy (ΔG) values can be obtained using Eq. (6):

$$\Delta G = \Delta H - T\Delta S. \tag{6}$$

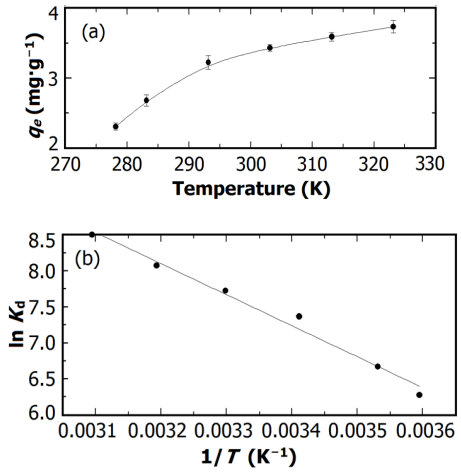

Fig. 4. Effect of temperature on Th biosorption by the living cells of *Bacillus* sp. dwc-2 (a) and variation of $\ln K_d$ with T^{-1} (b). (C_0 = 100 mg/L, M = 100 mg, V = 20 mL, pH = 3.0, t = 4 h)

The values of ΔH and ΔS, calculated from the slope and intercept of the plots of $\ln K_d$ versus T^{-1} (Fig. 4(b)), were listed in Table 2, and the values of ΔG were derived using Eq. (6). The positive ΔH value showed that the thorium biosorption was endothermic, and the positive value of ΔS revealed the increasing randomness during the biosorption process. The negative ΔG values indicates that the biosorption process is spontaneous, and the decrease of ΔG values with increasing temperature suggests that the thorium

TABLE 1. Parameters at 303.15 K for Langmuir and Freundlich isotherm models of Th biosorption by living cells of *Bacillus* sp. dwc-2

Microbe	Langmuir isotherm			Freundlich isotherm		
	q_m(mg/g)	b (L/mg)	R^2	K_F [(mg/g) (L/mg)$^{1/n}$]	n	R^2
Bacillus sp. dwc-2	11.42	0.2577	0.9930	1.8787	2.2012	0.9803

biosorption process may be more favorable at higher temperatures.

C. Biosorption mechanism involving thorium on *Bacillus* sp. dwc-2

1. SEM analysis

SEM was used to explore the microscopic behavior of microbial sorption. Figure 5 shows SEM images of the living cells before and after biosorption, surfaces of the cell after biosorption became very rough, with small granular material accumulated, and by EDS analysis the small granular material is thorium (Th^{4+}). SEM and EDS analysis was done with the dead cells, and the results (not shown) are quite the same as results of the living cells. Previous analyses indicated that the surface of microbial cells were rich in carboxyl, hydroxyl, and amino groups, which can bind nuclides via complexation or electrostatic interaction. Effect of pH on thorium biosorption implied that electrostatic interaction was an important mechanism. Consequently, we may conclude that the bacteria absorbed Th mainly via electrostatic interaction, which depends on the nature of the surface groups negatively charged. Meanwhile, we cannot rule out the possibility that the surface groups complexed Th^{4+}.

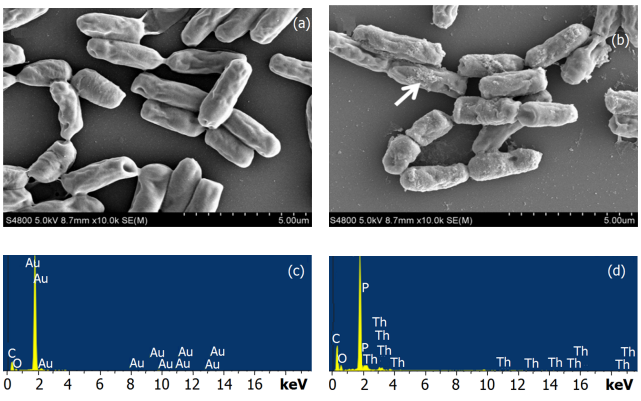

Fig. 5. (Color online) SEM images of living cells of *Bacillus* sp. dwc-2 before (a) and after (b) biosorption, and the relative EDS spectra (c and d). ($C_0 = 10\,\mathrm{mg\,L^{-1}}$, pH = 3.0, T = 303.15 K)

2. TEM analysis

Upon its biosorption by *Bacillus* sp. dcw-2, thorium ions may attach to the cell surface or migrate into the cell. Although most heavy metals are not needed for the life of microbes, some of them can indeed cross the cell membrane, via diffusion, nonspecific uptake system, or ion channels. Here TEM was employed to explore the topology of the cells after their biosorption of Th. The TEM images (Fig. 6) show that structures of living and dead cells changed differently after biosorption. From Figs. 6(a) and 6(b), the cells structures of living bacteria after biosorption were complete. Th absorbed did not enter into the center region of cells (white center region in Fig. 6(b)), and mainly deposited in the cytoplasm. For the dead bacteria, however, the cells structures were destroyed by autoclaving (Figs. 6(c) and 6(d)). As reported before [39, 40], metal binding to anionic functional groups on cell surface is a metal resistance and protection mechanism. In response to metal presence, the living microbes immobilize the toxic metal by extracellular materials and prevent it from entering into the cells. In contrast, the dead cell structure was destroyed and cannot immobilize the toxic metal. Therefore, thorium ions may enter into cytoplasm through osmosis, diffusion, or other pathways, but not being actively transported into cells [33]. In addition, in Fig. 6(b), many fine particles can be seen in the cells after the biosorption (the arrows). The particles could be Th, and they served as cores for growth of element precipitation (e.g., phosphate minerals) or by self-precipitation of hydroxides.

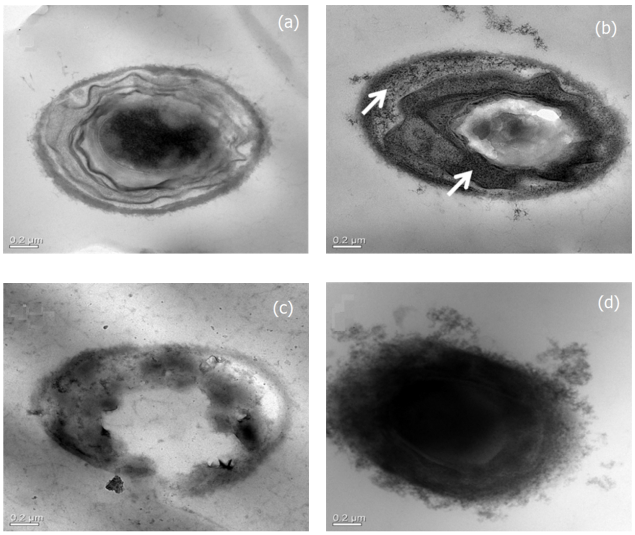

Fig. 6. TEM images of living cells of *Bacillus* sp. dwc-2 before (a) and after (b) biosorption, the dead cells before (c) and after (d) biosorption. ($C_0 = 10$ mg/L, pH = 3.0, $T = 303.15$ K)

TABLE 2. Thermodynamic parameters for Th biosorption by living cells of *Bacillus* sp. dwc-2

Microbe	ΔH (mg/g)	ΔS (mg/g)	ΔG (mg/g)					
			278.15 K	283.15 K	293.15 K	303.15 K	313.15 K	323.15 K
Bacillus sp. dwc-2	35.81	181.90	−14.78	−15.70	−17.52	−19.33	−21.15	−22.97

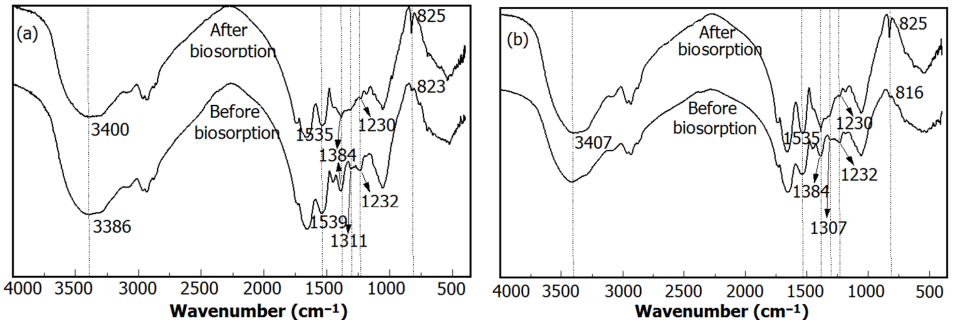

Fig. 7. FTIR spectra of the living (a) and dead (b) cells of *Bacillus* sp. dwc-2 before and after biosorption. (C_0 = 10 mg/L, pH = 3.0, T = 303.15 K)

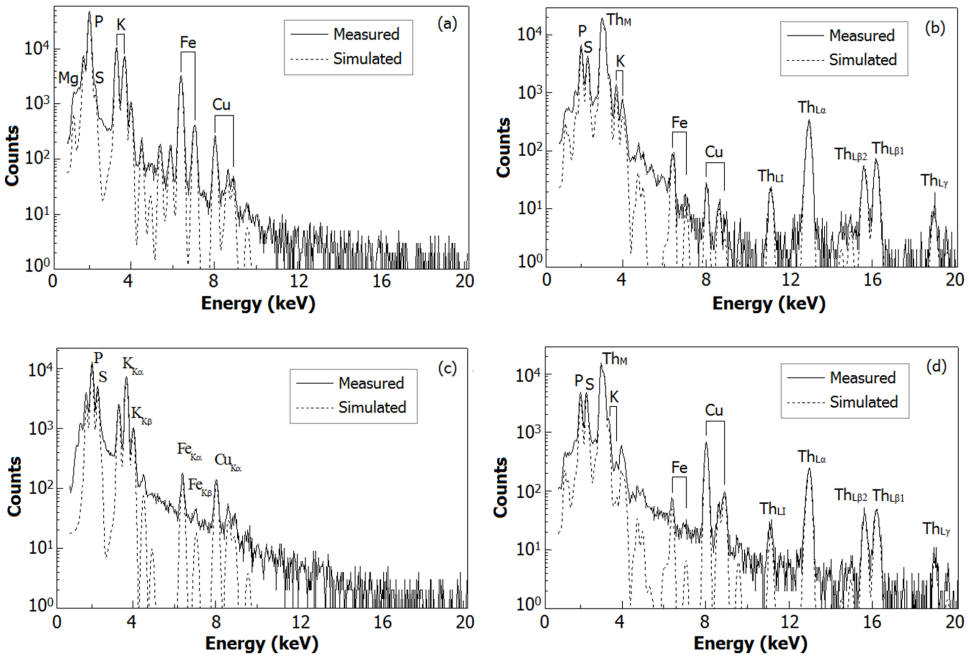

Fig. 8. PIXE spectra of the living cells of *Bacillus* sp. dwc-2 before (a) and after (b) biosorption, the dead cells before (c) and after (d) biosorption. (C_0 = 10 mg/L, pH = 3.0, T = 303.15 K)

3. *FTIR analysis*

Figure 7 shows FTIR spectra of living and dead cells before and after thorium biosorption. The FTIR spectra of living cells after biosorption were roughly identical to that of living cells before biosorption, and this was also true for the dead cells. The FTIR spectra of all the bacterial preparations had intense peaks at a frequency level of 3 400–3 200 cm^{-1} representing –OH stretching of carboxylic groups and also representing stretching of –NH groups [41]. All spectra for the bacterial samples, living or dead, revealed presence of protein related bands. The spectra after biosorption showed a peak shift from 3 386 cm^{-1} to 3 400 cm^{-1} in the living cells and a weakened peak intensity of the 3 407 cm^{-1} in the dead cells, which indicated the binding of thorium with hydroxyl and amino groups, namely protein. The γC=O of amide I and δNH/γC=O combination of the amide II bonds were prominent at ∼1 665 cm^{-1} and 1 545 cm^{-1}, respectively [33]. Compared to the original living cells, a minor shift from 1 539 cm^{-1} to 1 535 cm^{-1} and a strengthened peak intensity of the ∼1 728 cm^{-1} (C=O) [42], reflected

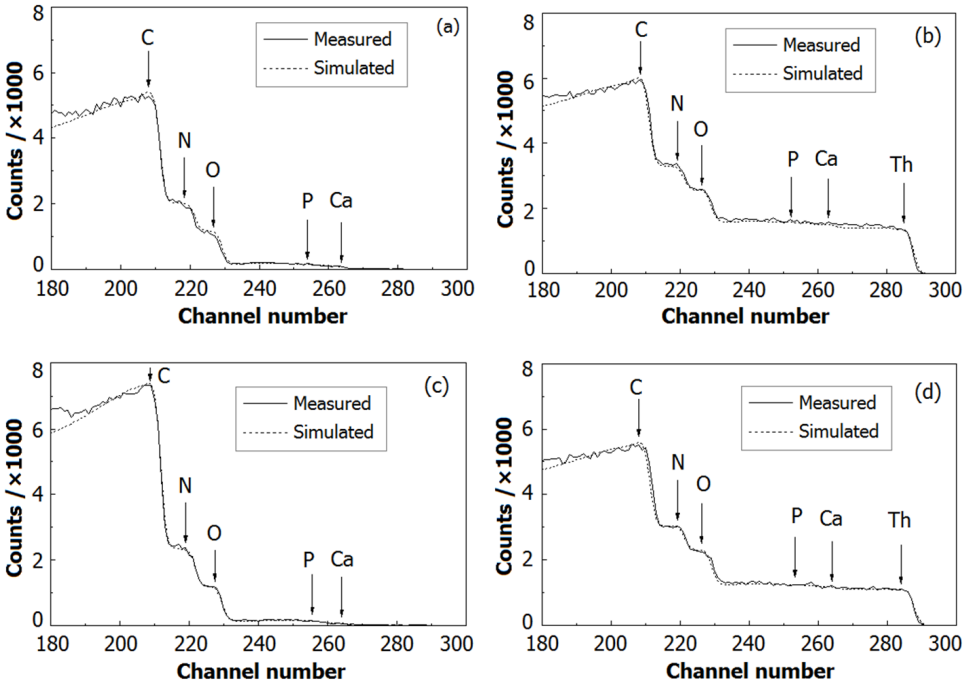

Fig. 9. EPBS spectra of the living cells of Bacillus sp. dwc-2 before (a) and after (b) biosorption, the dead cells before (c) and after (d) biosorption. ($C_0 = 10$ mg/L, pH $= 3.0$, $T = 303.15$ K)

some alteration in the secondary structure of cellular proteins. The peaks 1 384 cm^{-1} of the spectra after biosorption were significantly weakened, confirming the role of C(=O)−O^- stretching vibration [43], and the peaks at 1 307 or 1 311 cm^{-1} corresponding to stretching of non-ionized carboxylic groups (C−OH) disappeared [44]. The difference was due to the presence of carboxyl groups, and indicated the important role of carboxyl groups in thorium binding. The asymmetric stretching modes of protonated polyphosphates and $PO_{uncomplexed}$ in phosphate diesters have been shown to have strong absorption at around 1 240 cm^{-1} [45]. A decrease in intensity and a gradual shift at 1 232 cm^{-1} indicated the weakening of the P=O character as a result of thorium binding to the phosphates. The gradual peaks from 823 to 825 cm^{-1} in the living cells and from 816 to 825 cm^{-1} in the dead cells were due to phosphate functional groups [46], too. The overall spectral analysis strongly supported the major role of carboxyl, phosphate and protein in thorium binding by the bacterial biomass via complexation.

TABLE 3. Elemental contents of living and dead cells of *Bacillus* sp. dwc-2 before and after biosorption of Th, determined by PIXE

Bacillus sp. dwc-2		Elemental mass percentage (%)					
		Mg	P	S	K	Fe	Th
Living cells	Before adsorption	1.16	5.84	0.15	1.05	1.46	—
	After adsorption	—	1.04	0.46	0.07	0.05	26.61
Dead cells	Before adsorption	—	0.91	0.27	0.16	0.05	—
	After adsorption	—	0.73	0.54	0.04	0.03	20.31

TABLE 4. Elemental contents of living and dead cells of *Bacillus* sp. dwc-2 before and after biosorption of Th, determined by EPBS

Bacillus sp. dwc-2		Elemental mass percentage (%)					
		C	O	N	P	Ca	Th
Living cells	Before adsorption	57.06	17.34	13.78	2.49	2.32	—
	After adsorption	48.21	17.35	12.52	2.51	2.53	10.65
Dead cells	Before adsorption	63.80	12.64	13.31	1.68	1.37	—
	After adsorption	48.23	19.45	13.07	2.14	2.06	8.68

4. *PIXE and EPBS analyses*

PIXE and EPBS techniques were used to further investigate the biosorption mechanism. PIXE is a nondestructive, simultaneous trace multi-element analytical technique [47, 48]. Depending on proton energy and sample preparation, detection limits may be as low as μg/g with common figures in the mg/g range [49]. However, few reports of PIXE analyses of metal-adsorbed microorganisms were identified prior to this study. Based on these precedents, we used PIXE to analyze the elemental change in *Bacillus* sp. dwc-2 before and after biosorption. Considering PIXE cannot determine light elements, we combined EPBS and PIXE tests to better observe the full elemental composition. As showed in Figs. 8 and 9, after biosorption thorium peaks can be seen in the PIXE and EPBS spectra (Figs. 8(b) and 8(d), Figs. 9(b) and 9(d)), which were not detected before biosorption (Figs. 8(a) and 8(c), Figs. 9(a) and 9(c)). It demonstrated that Th was absorbed by *Bacillus* sp. dwc-2.

The element mass percentages of living and dead cells before and after biosorption were calculated from the PIXE

and EPBS spectra to provide a quantitative analysis (Tables 3 and 4). Some reports also used PIXE to investigate biosorption as an analytical technique [50, 52–54], but they tended to get results through qualitative analysis rather than quantitative analysis. Our PIXE results showed that the amounts of K^+, Mg^{2+} and Fe^{3+} decreased to different extents after biosorption, especially Mg^{2+}, which almost disappeared completely. These ions might be replaced by Th^{4+} via ion-exchange. According to the literature [5], the size and charge of cation helps to determine the strength of biosorption. In their excess presence, thorium ions may initially compete for the limited number of cation sorption sites presented in *Bacillus* sp. dwc-2 by replacing less charged cations such as K^+, Mg^{2+} and Fe^{3+}. The above analysis indicated that ion-exchange was also a biosorption pathway for thorium.

IV. CONCLUSION

The biosorption of thorium on *Bacillus* sp. dwc-2 was a complicated process controlled by many environmental variables such as pH, contact time, temperature, thorium and biomass concentration. In the presence of bacteria, the biosorption of thorium was a pH-dependent process and certain amounts of thorium were quickly adsorbed onto bacteria. The biosorption experiments indicated that thorium biosorption had an optimum pH of 3.0 and a maximum sorption capacity of 10.75 mg/g (wet wt.). The living cells need more time (4 h) to reach equilibrium than dead cells (5 min). Electrostatic interaction was a major driving force for the biosorption. The biosorption agreed better with the Langmuir isotherm model than the Freundlich model, indicating that the Th biosorption formed a monolayer coverage. The thermodynamic parameters, negative change in Gibbs free energy, and positive value in enthalpy and entropy, revealed that the biosorption was spontaneous, more favorable at higher temperature and endothermic process with an increase of entropy. SEM-EDS analysis showed that small granular material adsorbed on the cell surface was likely to be thorium ions. TEM analysis revealed that the structures of living and dead cells were different. For the living bacteria, their cells structures after biosorption were complete, not be destroyed and Th absorbed mainly deposited in the cytoplasm served as cores for growth of element precipitation (e.g., phosphate minerals) or by self-precipitation of hydroxides, and could not enter into the center region of cells. Meanwhile, for the dead bacteria, their structures were destroyed by autoclaving at 394.15 K and Th can enter into the center region of cells. FTIR analysis combined with biosorption experiments further indicated that thorium biosorption on cells were associated with carboxyl, phosphate and protein, and might be governed by complexation or electrostatic interaction. In addition, PIXE and EPBS analyses showed that K^+, Mg^{2+} and Fe^{3+} were replaced by Th^{4+} (ion-exchange). These results indicated that electrostatic interaction, complexation, and ion-exchange could be involved in thorium biosorption by this bacterium. Our findings in biosorption of thorium-*Bacillus* sp. dwc-2 system have established a strong basis for future investigation and modeling of microbe-based bioremediation strategies to clean up thorium-contaminated sites.

ACKNOWLEDGEMENTS

We would like to thank Prof. WANG Dong-Qi, Multidisciplinary Initiative Center, Institute of High Energy Physics, Chinese Academy of Sciences, China, for his enthusiastic help in our manuscript writing.

[1] Tsezos M and Volesky B. Biosorption of uranium and thorium. Biotechnol Bioeng, 1981, **23**: 583–604. DOI: 10.1002/bit.260230309
[2] Csom Gy, Reiss T, Fehér S, *et al*. Thorium as an alternative fuel for SCWRs. Ann Nucl Energy, 2012, **41**: 67–78. DOI: 10.1016/j.anucene.2011.11.007
[3] Lloyd J R and Renshaw J C. Bioremediation of radioactive waste: radionuclide-microbe interactions in laboratory and field-scale studies. Curr Opin Biotech, 2005, **16**: 254–260. DOI: 10.1016/j.copbio.2005.04.012
[4] Lloyd J R and Macaskie L E. Bioremediation of radionuclide-containing wastewaters. Washington, DC: ASM Press, 2000.
[5] Maier R M, Pepper I L, Gerba C P. Environmental microbiology. Access Online via Elsevier; 2009.
[6] Wang J L and Chen C. Biosorbents for heavy metals removal and their future. Biotechnol Adv, 2009, **27**: 195–226. DOI: 10.1016/j.biotechadv.2008.11.002
[7] Gadd G M. Biosorption: critical review of scientific rationale, environmental importance and significance for pollution treatment. J Chem Technol Biot, 2009, **84**: 13–28. DOI: 10.1002/jctb.1999
[8] Vijayaraghavan K and Yun Y S. Bacterial biosorbents and biosorption. Biotechnol Adv, 2008, **26**: 266–291. DOI: 10.1016/j.biotechadv.2008.02.002
[9] Volesky B. Biosorption and me. Water Res, 2007, **41**: 4017–4029. DOI: 10.1016/j.watres.2007.05.062
[10] Mack C, Wilhelmi B, Duncan J R, *et al*. Biosorption of precious metals. Biotechnol Adv, 2007, **25**: 264–271. DOI: 10.1016/j.biotechadv.2007.01.003
[11] Gavrilescu M. Removal of heavy metals from the environment by biosorption. Eng Life Sci, 2004, **4**: 219–232. DOI: 10.1002/elsc.200420026
[12] Andrès Y, Texier A C and Le Cloirec P. Rare earth elements removal by microbial biosorption: a review. Environ Technol, 2003, **24**: 1367–1375. DOI: 10.1080/09593330309385681
[13] Volesky B and Holan Z R. Biosorption of heavy metals. Biotechnol Progr, 1995, **11**: 235–250. DOI: 10.1021/bp00033a001
[14] Wang J L and Chen C. Biosorption of heavy metals by *Saccharomyces cerevisiae*: A review. Biotechnol Adv, 2006, **24**: 427–451. DOI: 10.1016/j.biotechadv.2006.03.001

[15] Haas J, Dichristina T J and Wade R. Thermodynamics of U(VI) sorption onto *Shewanellaputrefaciens*. Chem Geol, 2001, **180**: 33–54. DOI: 10.1016/S0009-2541(01)00304-7

[16] Tabak H H, Lens P, van Hullebusch E D, *et al*. Developments in bioremediation of soils and sediments polluted with metals and radionuclides – 1. Microbial processes and mechanisms affecting bioremediation of metal contamination and influencing metal toxicity and transport. Rev Environ Sci Bio, 2005, **4**: 115–156. DOI: 10.1007/s11157-005-2169-4

[17] Schiewer S and Volesky B. Biosorption processes for heavy metal removal. Environmental microbe-metal interactions. Washington DC: ASM Press, 2000, 329–362.

[18] Lan T, Feng Y, Liao J, *et al*. Biosorption behavior and mechanism of cesium-137 on *Rhodosporidium fluviale* strain UA2 isolated from cesium solution. J Environ Radioactiv, 2014, **134**: 6–13. DOI: 10.1016/j.jenvrad.2014.02.016

[19] Kazy S K, Das S K and Sar P. Lanthanum biosorption by a *Pseudomonas* sp.: equilibrium studies and chemical characterization. J Ind Microbiol Biot, 2006, **33**: 773–783. DOI: 10.1007/s10295-006-0108-1

[20] Yong P and Macaskie L E. Bioaccumulation of lanthanum, uranium and thorium, and use of a model system to develop a method for the biologically-mediated removal of plutonium from solution. J Chem Technol Biot, 1998, **71**: 15–26. DOI: 10.1002/(SICI)1097-4660(199801)71:1<15::AID-JCTB773>3.0.CO;2–8

[21] Sar P and D'Souza S F. Biosorption of thorium (IV) by a *Pseudomonas* biomass. Biotechnol Lett, 2002, **24**: 239–243. DOI: 10.1023/A:1014153913287

[22] Nakajima A and Tsuruta T. Competitive biosorption of thorium and uranium by *Micrococcus luteus*. J Radioanal Nucl Ch, 2004, **260**: 13–18. DOI: 10.1023/B:JRNC.0000027055.16768.1e

[23] Tsuruta T. Cell-associated adsorption of thorium or uranium from aqueous system using various microorganisms. Water Air Soil Poll, 2004, **159**: 35–47. DOI: 10.1023/B:WATE.0000049190.05993.3b

[24] Tsuruta T. Bioaccumulation of uranium and thorium from the solution containing both elements using various microorganisms. J Alloy Compd. 2006, **408**: 1312–1315. DOI: 10.1016/j.jallcom.2005.04.131

[25] Picardo M C, Ferreira A C d M and da Costa A C A. Continuous thorium biosorption-dynamic study for critical bed depth determination in a fixed-bed reactor. Bioresource Technol, 2009, **100**: 208–210. DOI: 10.1016/j.biortech.2008.05.047

[26] Picardo M C, Ferreira A C d M and da Costa A C A. Biosorption of radioactive thorium by *Sargassum filipendula*. Appl Biochem Biotech, 2006, **134**: 193–206. DOI: 10.1385/ABAB:134:3:193

[27] Ozdemir S, Erdogan S and Kilinc E. *Bacillus* sp. immobilized on Amberlite XAD-4 resin as a biosorbent for solid phase extraction of thorium prior to UV-vis spectrometry determination. Microchim Acta, 2010, **171**: 275–281. DOI: 10.1007/s00604-010-0423-0

[28] Elwakeel K Z, El-Sadik H A, Abdel-Razek A S, *et al*. Environmental remediation of thorium (IV) from aqueous medium onto *Cellulosimicrobium cellulans* isolated from radioactive wastewater. Desalin Water Treat, 2012, **46**: 1–9. DOI: 10.1080/19443994.2012.67405

[29] Ozdemir S, Okumuş V, Dündar A, *et al*. The use of fungal biomass *Agaricus bisporus* immobilized on amberlite XAD-4 resin for the solid-phase preconcentration of thorium. Bioremediat J, 2014, **18**: 38–45. DOI: 10.1080/10889868.2013.834870

[30] Tsezos M and Volesky B. The mechanism of thorium biosorption by *Rhizopus arrhizus*. Biotechnol Bioeng, 1982, **24**: 955–969. DOI: 10.1002/bit.260240415

[31] Santamaría M, Díaz-Marrero AR, Hernández J, *et al*. Effect of thorium on the growth and capsule morphology of *Bradyrhizobium*. Environ Microbiol, 2003, **5**: 916–924. DOI: 10.1046/j.1462-2920.2003.00487.x

[32] Díaz-Marrero A R, Santamaría M, Hernández J, *et al*. Coprecipitation of Th^{4+} and the purified extracellular polysaccharide produced by bacterium *Bradyrhizobium* (*Chamaecytisus*) BGA-1. Appl Microbiol Biot, 2004, **65**: 356–362. DOI: 10.1007/s00253-004-1631-5

[33] Kazy S, D'Souza S F and Sar P. Uranium and thorium sequestration by a *Pseudomonas* sp.: Mechanism and chemical characterization. J Hazard Mater, 2009, **163**: 65–72. DOI: 10.1016/j.jhazmat.2008.06.076

[34] Khan M H, Ali A and Khan N N. Spectrophotometric determination of thorium with disodium salt of Arsenazo-III in perchloric acid. J Radioanal Nucl Ch, 2001, **250**: 353–357. DOI: 10.1023/A:1017968217578

[35] Tatzber M, Stemmer M, Spiegel H, *et al*. An alternative method to measure carbonate in soils by FT-IR spectroscopy. Environ Chem Lett, 2007, **5**: 9–12. DOI: 10.1007/s10311-006-0079-5

[36] Tsuruta T. Accumulation of thorium ion using various microorganisms. J Gen Appl Microbiol, 2003, **49**: 215–218. DOI: 10.2323/jgam.49.215

[37] Ding C, Feng S, Cheng W, *et al*. Biosorption behavior and mechanism of thorium on *Streptomyces sporoverrucosus* dwc-3. J Radioanal Nucl Ch, 2014, **301**: 237–245. DOI: 10.1007/s10967-014-3110-5

[38] Bhainsa K C and D'Souza S F. Thorium biosorption by Aspergillus fumigatus, a filamentous fungal biomass. J Hazard Mater, 2009, **165**: 670–676. DOI: 10.1007/s10967-014-3110-5

[39] Beveridge T and Koval S. Binding of metals to cell envelopes of Escherichia coli K-12. Appl Environ Microb, 1981, **42**: 325–335.

[40] Merroun M L, Ben Chekroun K, Arias J M, *et al*. Lanthanum fixation by *Myxococcus xanthus*: cellular location and extracellular polysaccharide observation. Chemosphere, 2003, **52**: 113–120. DOI: 10.1016/S0045-6535(03)00220-0

[41] Pang C, Liu Y, Cao X, *et al*. Biosorption of uranium (VI) from aqueous solution by dead fungal biomass of *Penicillium citrinum*. Chem Eng J, 2011, **170**: 1–6. DOI: 10.1016/j.cej.2010.10.068

[42] Pan J H, Liu R X and Tang H X. Surface reaction of *Bacillus cereus* biomass and its biosorption for lead and copper ions. J Environ Sci, 2007, **19**: 403–408. DOI: 10.1016/S1001-0742(07)60067-9

[43] Pang C, Liu Y H, Cao X H, *et al*. Biosorption of uranium (VI) from aqueous solution by dead fungal biomass of Penicillium citrinum. Chem Eng J, 2011, **170**: 1–6. DOI: 10.1016/j.cej.2010.10.068

[44] Martins M, Faleiro M L, da Costa A M R, *et al*. Mechanism of uranium (VI) removal by two anaerobic bacterial communities. J Hazard Mater, 2010, **184**: 89–96. DOI: 10.1016/j.jhazmat.2010.08.009

[45] Jiang W, Saxena A, Song B, *et al*. Elucidation of functional groups on gram-positive and gram-negative bacterial surfaces using infrared spectroscopy. Langmuir, 2004, **20**: 11433–11442. DOI: 10.1021/la049043+

[46] García-Mendieta A, Olguín M T and Solache-Ríos M. Biosorption properties of green tomato husk (Physalis philadelph-

ica Lam) for iron, manganese and iron-manganese from aqueous systems. Desalination, 2012, **284**: 167–174. DOI: 10.1016/j.desal.2011.08.052

[47] Goodall W R, Scales P J and Ryan C G. Applications of PIXE and diagnostic leaching in the characterisation of complex gold ores. Miner Eng, 2005, **18**: 1010–1019. DOI: 10.1016/j.mineng.2005.01.011

[48] Ghazvini P T M and Mashkani S G. Screening of bacterial cells for biosorption of oxyanions: Application of micro-PIXE for measurement of biosorption. Hydrometallurgy, 2009, **96**: 246–252. DOI: 10.1016/j.hydromet.2008.10.012

[49] Rodriguezlugo V, Miranda J, Viquez S, *et al*. Application of PIXE and XRD to the characterization of clays. Microchem J, 1995, 52: 356–363. DOI: 10.1006/mchj.1995.1108

[50] Mashkani S G and Ghazvini P T M. Biotechnological potential of *Azolla filiculoides* for biosorption of Cs and Sr: application of micro-PIXE for measurement of biosorption. Bioresource Technol, 2009, **100**: 1915–1921. DOI: 10.1016/j.biortech.2008.10.019

[51] Espinoza-Quinoñes F, Rizzutto M, Added N, *et al*. PIXE analysis of chromium phytoaccumulation by the aquatic macrophytes *Eicchornia crassipes*. Nucl Instrum Meth B, 2009, **267**: 1153–1157. DOI: 10.1016/j.nimb.2009.02.050

[52] Ghazvini P T M and Mashkani S G. Effect of salinity on vanadate biosorption by *Halomonas* sp. GT-83: preliminary investigation on biosorption by micro-PIXE technique. Bioresource Technol. 2009, **100**: 2361–2368. DOI: 10.1016/j.biortech.2008.11.025

[53] Kozai N, Ohnuki T, Sakamoto F, *et al*. Accumulation of Co in yeast cells under metabolically active condition-implication for role of yeast in migration of radioactive Co. J Nucl Sci Technol, 2011, **48**: 1206–1213. DOI: 10.1080/18811248.2011.9711808

[54] Laurette J, Larue C, Mariet C, *et al*. Influence of uranium speciation on its accumulation and translocation in three plant species: Oilseed rape, sunflower and wheat. Environ Exp Bot, 2012, **77**: 96–107. DOI: 10.1016/j.envexpbot.2011.11.007